

Collective optical excitation of interacting localized electrons

C. Metzner and G. H. Döhler

Institut für Technische Physik I, Universität Erlangen, Erwin-Rommel-Strasse 1, 91058 Erlangen, Germany

(Received 22 March 1999; revised manuscript received 9 June 1999)

We investigate theoretically the role of dynamic screening in the intersubband absorption process of a quasi-two-dimensional (quasi-2D) electron gas with in-plane localization caused by a strong disorder potential. Due to a correlation effect in the single-particle spectrum this system is equivalent to an array of randomly distributed, localized oscillators, which are mutually coupled by the electron-electron Coulomb interaction. In the limit of low-electron density, a broad absorption spectrum reflects the disorder-induced distribution of the individual transition energies. For increasing electron filling factor we find a depolarization-type blueshift similar to the case of quasi-2D systems without disorder. Simultaneously a dramatic line narrowing is observed, indicating a collective response of the interacting localized electrons. In this collective mode large clusters of mutually phase-adapted oscillators are formed in the layer plane. Our results are relevant for the interpretation of intraband absorption experiments in all kinds of disordered quasi-2D systems and in dense arrays of artificial quantum dots. A similar effect is expected for inter-Landau-level transitions in magnetically quantized 2D systems. [S0163-1829(99)06539-X]

I. INTRODUCTION

Optically induced intersubband (IS) transitions are the most characteristic excitations of quasi-two-dimensional (quasi-2D) electron systems. Their theoretical description involves many key concepts of modern semiconductor physics, like coherent interaction with a light field, many particle effects, disorder and ultrafast relaxation dynamics. These processes represent, however, not only a fascinating field of fundamental research, but also form the basis of many promising applications, like infrared detectors,¹ modulators,² lasers,³ and nonlinear devices.^{4,5}

In order to optimize the design of such structures, it is essential to have a quantitative theory of the factors that determine, for example, the peak position and line shape of the optical intersubband spectrum. In the present understanding, these features result from an interplay of collective polarization and various broadening mechanisms.

It is now well established that the experimentally observed intersubband resonance is (at least for the usual carrier densities) a collective, plasmonlike response of the interacting electron gas and in general cannot be described in terms of single-particle transitions. The importance of many-particle effects shows up most clearly in the density-dependent shift of the resonance peak position $\hbar\omega_{max}$ (relative to the subband separation $\epsilon_{10} = \epsilon_1 - \epsilon_0$), which has been explained by the depolarization field and excitonlike final-state interactions.⁶⁻¹¹ In addition, it has been shown that nonparabolicity¹² of the electronic subbands, which would in a single-particle picture yield a broad absorption spectrum, need not to be observable in an experiment, because the many-particle interactions tend to concentrate all oscillator strength into a narrow, collective mode.¹³⁻¹⁶ Thus, strictly speaking, it is not possible to infer the broadening mechanisms acting in a sample by simply measuring the absorption line width, especially when a depolarization blueshift of the peak indicates strong electron-electron interactions.

Despite these complications, the finite width of IS lines is

usually ascribed to the various broadening mechanisms in semiconductor heterostructures, like interface,¹⁷ charged impurity¹⁸ or alloy scattering and phonon emissions. Traditionally these mechanisms are divided into two classes called "homogeneous," i.e., equally acting on each elementary oscillator, and "inhomogeneous," i.e., resulting in differences between these oscillators. The relative importance of the two types is experimentally determined by comparing the line shape of the observed IS spectrum with a Lorentzian (indicating homogeneous broadening) and a Gaussian (characteristic for inhomogeneous broadening). Indeed there is experimental evidence that supports these ideas by demonstrating that removal of the charged impurities from the active part of the structure results in a considerable line narrowing¹⁹ and a gradual change from more Gaussian to more Lorentzian shape.²⁰ In such modulation-doped samples, the predominant broadening mechanism is normally interface roughness scattering. The linewidth of the Lorentzian can be further reduced by increasing the well width (weaker sensitivity for interface fluctuations)²¹ and in some cases even approaches the theoretical limit determined by optical phonon emissions.²² There is thus a tendency to believe that inhomogeneous broadening (structural disorder) plays no more significant role in high-quality samples.

Recently, more refined methods like fitting with a Voigt profile, or saturation spectroscopy, have revealed an inhomogeneous contribution to the IS linewidth in samples, where the line shape was in between the two prototypes.²³ However, the clearest way to separate both contributions is probably by hole burning spectroscopy. Such measurements have convincingly demonstrated that homogeneous and inhomogeneous broadening can be of comparable magnitude, even in modulation-doped samples.²⁴ The observed spectrum is actually a superposition of many relatively narrow Lorentzians, centered at different photon energies. Physically speaking, the system behaves like an inhomogeneous collection of individual oscillators with a random distribution of resonance frequencies.

Yet, underlying the prevalent picture of IS transitions there is still the concept of free electrons moving parallel to the layers and being only sometimes interrupted by an elastic or inelastic scattering events. Consequently, these processes are characterized by a momentum (T_2) and energy relaxation time (T_1).

Indeed, in a structurally perfect sample (no doping, interface, or alloy disorder), the lifetime of the excited (plane-wave like) electron state would be limited by phonon-assisted relaxation and this should result in a Lorentzian IS line. However, as soon as structural disorder is introduced into the system, coherent multiple elastic scattering of the carriers with the static imperfections will fundamentally change the electronic single-particle wavefunctions. In most realistic situations, a part of the electrons will become strongly localized in the layer plane. Even if the random potential created by the disorder is too weak or too-short range to cause strong localization, the (to a certain degree) extended electron wave functions will, nevertheless, be modulated in the plane with a complex pattern of local scattering resonances. Therefore, disorder is not merely a small perturbation on the free 2D electron gas, but requires to adopt a completely different theoretical viewpoint of the system.

In this paper, we will present a model of the IS resonance on the basis of disorder-localized single-particle states, including dynamic effects of the electron-electron interaction. The organization of the paper is as follows. In Sec. II, our general concept is outlined with reference to our earlier work on this field. In Sec. III, a ‘‘localized version’’ of IS depolarization theory is developed. For its efficient numerical evaluation, a simple model system is introduced in Sec. IV and the results of the calculations are presented in Sec. V. We summarize in Sec. VI. Finally, in Sec. VII, we discuss possible extensions and applications of our theory in related parts of physics.

II. GENERAL CONCEPT

The theoretical analysis of IS transitions in strongly disordered systems is considerably complicated by the additional lateral (x, y -) localization of the electron states. Neither the subband index m (subband mixing), nor the lateral wave vector \vec{k} (no more free motion parallel to the layers) can be considered as good quantum numbers any longer. The homogeneous film of electrons is decomposed into a random array of ‘‘drops’’ or ‘‘natural quantum dots.’’ To obtain realistic results in this situation, it is clearly insufficient to include the disorder only phenomenologically by some ‘‘broadening parameter.’’ Instead, the theory should be based from the start on single-particle states $|l\rangle$ of the general form $\varphi^{(l)}(\vec{R}) = \sum_m f_m(z) g_m^{(l)}(x, y)$, with z -subband wave functions $f_m(z)$ and localized lateral functions $g_m^{(l)}(x, y)$.

Recently, exact diagonalization studies of this kind have been published for the case of modulation-doped quantum wells²⁵ and doping superlattices,²⁶ including several subbands (i.e., $m=0 \dots M$ with $M \geq 1$). Despite a drastic disorder broadening of the density of states (of order 100 meV), it turned out that the spectrum of localized quantum states $|l\rangle$ can be divided into ‘‘correlated groups,’’ $\{|l\rangle\} \rightarrow \{ \{ |(i)0\rangle, |(i)1\rangle, \dots |(i)M\rangle \}, \{ |(j)0\rangle, |(j)1\rangle, \dots |(j)M\rangle \},$

$\dots \}$. The groups (i) , (j) , and so on constitute the above mentioned natural quantum dots. All states $|(i)m\rangle$ belonging to dot (i) are localized in the same lateral region, typically at a local minimum of the disorder potential. They share a very similar lateral structure and differ from each other by the specific subband m from which they (mainly) descent. Their difference of eigenenergies is close to the subband spacing of the undisturbed (i.e., without disorder) system, $\epsilon_{mn}^{(i)} = \epsilon_{(i)m} - \epsilon_{(i)n} \approx \epsilon_{mn}$. This is a quantum-mechanical formulation of the intuitive semiclassical picture of local subband edges $\epsilon_m(x, y)$ that fluctuate strongly but ‘‘in parallel.’’ If such a system is excited with light polarized in z direction, transitions are induced almost exclusively between correlated (intradot) states (‘‘vertical transitions in real space’’) and correspondingly the absorption line is much narrower than the broad density of states would suggest.

So far, the IS transitions in strongly localized systems have been calculated without any electron-electron interaction,²⁵ or with the inclusion of only static screening.²⁶ In this paper, we investigate the role of dynamic many-particle effects for the IS absorption process on the basis of the previous single-particle results.

III. THEORY

The correlation effect in the one-particle spectrum leads to a scenario of randomly located quantum dots (i) , each of which contains (at least) two strongly localized states $|(i)0\rangle$ and $|(i)1\rangle$. An electron occupying this quantum dot will perform resonant transitions between the two correlated states, if an electric ac field (the excitation light) of suitable frequency $\omega \approx \epsilon_{10}^{(i)}/\hbar$ is applied along the z direction. This corresponds in real space to an oscillation of the electron in z direction within its associated quantum dot. Thus, each (occupied) dot acts as a localized two-level oscillator. Since electrons can relax from their excited state via phonon emission, the oscillators have a finite damping and thus energy is continuously absorbed from the light field. The individual resonance frequencies $\epsilon_{10}^{(i)}/\hbar$ of the oscillators are different due to the disorder.

In the independent particle approximation the absorption spectrum of the whole system simply reflects the dispersion of these $\epsilon_{10}^{(i)}$. However, the oscillating charge density in each dot causes a fluctuating (long-range) Coulomb potential, which couples the motion of all electrons and opens the possibility of collective many-body effects. In the following we describe this dynamic electron-electron interaction on the level of the time-dependent Hartree approximation.

The z -polarized excitation light beam is described by a homogeneous electric field $F(t)$ with harmonic time dependence,

$$F(t) = F \vec{e}_z \cos(\omega t), \quad (1)$$

acting on the electrons as an external potential (energy):

$$W^{ext}(\vec{R}, t) = (-e) F z \cos(\omega t). \quad (2)$$

In response, the electrons create an induced Coulomb potential,

$$W^{ind}(\vec{R}, t) = \sum_i V^{(i)}(\vec{R}, t), \quad (3)$$

where $V^{(i)}(\vec{R}, t)$ is the individual contribution of localized oscillator (i). The total time-dependent potential prevailing in the system is then

$$W(\vec{R}, t) = W^{ext}(\vec{R}, t) + W^{ind}(\vec{R}, t). \quad (4)$$

In the linear response regime, no frequency components are produced except those contained in the excitation light. Thus, we can decompose the monochromatic total potential into two temporal Fourier components. Note that in our disordered system, the modulus and relative phase shift of the resulting field will both have a complicated position dependence:

$$W(\vec{R}, t) = W(\vec{R}, \omega) e^{i\omega t} + W^*(\vec{R}, \omega) e^{-i\omega t} \quad (5)$$

$$= 2|W(\vec{R}, \omega)| \cos[\omega t + \Delta\varphi(\vec{R}, \omega)], \quad (6)$$

where $\Delta\varphi(\vec{R}, \omega)$ is the phase of complex number $W(\vec{R}, \omega)$. The ω component of the total potential experienced by oscillator (i) is given by

$$W^{(i)}(\vec{R}, \omega) = \frac{-eFz}{2} + \sum_{j \neq i} V^{(j)}(\vec{R}, \omega), \quad (7)$$

where we have explicitly excluded self interaction. Here $V^{(j)}(\vec{R}, \omega)$ is the temporal Fourier transform of $V^{(j)}(\vec{R}, t)$.

We now calculate the linear response of oscillator (i) to this perturbation, assuming that initially (i.e., without excitation) the electron is in the ground state (i0) and the excited state (i1) is unoccupied. A small phenomenological damping term Γ (with dimension of energy) is introduced to account for homogeneous phonon broadening. We can expand the time-dependent wave function in terms of the localized eigenstates

$$\Psi^{(i)}(\vec{R}, t) = \sum_m b_m^{(i)}(\omega, t) \varphi_m^{(i)}(\vec{R}). \quad (8)$$

Following the usual procedure of first-order time-dependent perturbation theory and neglecting the terms oscillating with the natural frequencies

$$\Delta\omega_{m0}^{(i)} = \omega_m^{(i)} - \omega_0^{(i)}, \quad (9)$$

the coefficients in Eq. (8) are found to have the same frequency components as the excitation field

$$b_m^{(i)}(\omega, t) = c_m^{(i)}(+\omega) e^{+i\omega t} + c_m^{(i)}(-\omega) e^{-i\omega t}. \quad (10)$$

The two components $c_m^{(i)}$ differ only by the sign of ω , describing resonant ($-\omega$) and anti-resonant ($+\omega$) excitation. They are given by an expression well known from time-dependent random phase approximation theory

$$c_m^{(i)}(\omega) = \frac{-\langle im | W^{(i)}(\vec{R}, \omega) | i0 \rangle}{\hbar[\Delta\omega_{m0}^{(i)} + \omega - i(\Gamma/\hbar)]}. \quad (11)$$

The induced space charge fluctuation is easily found from the wave function by

$$\rho^{(i)}(\vec{R}, t) = (-e)[|\Psi^{(i)}(\vec{R}, t)|^2 - |\varphi_0^{(i)}(\vec{R})|^2]. \quad (12)$$

Neglecting terms of order $O(W^2)$ (linear response) and anti-resonant terms (which are small for $\omega \approx \Delta\omega_{m0}^{(i)}$) one obtains

$$\rho^{(i)}(\vec{R}, t) = \sum_m (-e) \varphi_m^{(i)*}(\vec{R}) \varphi_0^{(i)}(\vec{R}) c_m^{(i)*}(-\omega) e^{i\omega t} + \text{c.c.} \quad (13)$$

From now on, we disregard all higher excited states $m > 1$ and treat each oscillator as a two-level system. Using the fact that the potential $W^{(i)}(\vec{R}, t)$ is real, we further rewrite the resonant coefficient in the following form:

$$c_1^{(i)*}(-\omega) = \left\{ \frac{-\langle i1 | W^{(i)}(\vec{R}, -\omega) | i0 \rangle}{\hbar[\Delta\omega_{10}^{(i)} - \omega - i(\Gamma/\hbar)]} \right\}^* \quad (14)$$

$$= \frac{\langle i0 | W^{(i)}(\vec{R}, \omega) | i1 \rangle}{\hbar[\omega - \Delta\omega_{10}^{(i)} - i(\Gamma/\hbar)]}. \quad (15)$$

It will be useful later to define a *response function* $p^{(i)}(\omega)$ of oscillator (i)

$$p^{(i)}(\omega) = \{\hbar[\omega - \Delta\omega_{10}^{(i)} + i(\Gamma/\hbar)]\}^{-1} \quad (16)$$

and its *spatial form factor* $\rho_0^{(i)}(\vec{R})$

$$\rho_0^{(i)}(\vec{R}) = (-e) \varphi_1^{(i)*}(\vec{R}) \varphi_0^{(i)}(\vec{R}). \quad (17)$$

Further, we introduce a dimensionless *excitation amplitude* $u^{(i)}(\omega)$

$$u^{(i)}(\omega) = p^{(i)}(\omega) \langle i0 | W^{(i)}(\vec{R}, \omega) | i1 \rangle. \quad (18)$$

In terms of these definitions, the induced space charge fluctuation of oscillator (i) can be written in compact form as

$$\rho^{(i)}(\vec{R}, \omega) = \rho_0^{(i)}(\vec{R}) u^{(i)}(\omega). \quad (19)$$

In order to calculate the corresponding potential, we use the Coulomb-Greens function

$$T(\vec{R} - \vec{R}') = \frac{-e}{4\pi\epsilon\epsilon_0} \frac{1}{|\vec{R} - \vec{R}'|}. \quad (20)$$

The ω component of the potential induced by oscillator (i) is then given by

$$V^{(i)}(\vec{R}, \omega) = \int d^3R' T(\vec{R} - \vec{R}') \rho^{(i)}(\vec{R}', \omega). \quad (21)$$

With the abbreviation

$$T^{(i)}(\vec{R}) = \int d^3R' T(\vec{R} - \vec{R}') \rho_0^{(i)}(\vec{R}') \quad (22)$$

this can be further simplified to

$$V^{(i)}(\vec{R}, \omega) = T^{(i)}(\vec{R}) u^{(i)}(\omega). \quad (23)$$

We now return to the potential experienced by oscillator (i), given by Eq. (7) and rewrite it in terms of the newly introduced quantities

$$W^{(i)}(\vec{R}, \omega) = \frac{-eFz}{2} + \sum_{j \neq i} T^{(j)}(\vec{R}) u^{(j)}(\omega). \quad (24)$$

According to Eq. (18), the response of oscillator (i) depends on the matrix elements of potential $W^{(i)}(\vec{R}, \omega)$ in the eigensubspace (i),

$$\begin{aligned} \langle i0 | W^{(i)}(\vec{R}, \omega) | i1 \rangle &= \frac{-eF}{2} \langle i0 | z | i1 \rangle \\ &+ \sum_{j \neq i} \langle i0 | T^{(j)}(\vec{R}) | i1 \rangle u^{(j)}(\omega) \end{aligned} \quad (25)$$

$$= \frac{-eF}{2} z^{(i)} + \sum_{j \neq i} T_{(i)}^{(j)} u^{(j)}(\omega), \quad (26)$$

where we have introduced abbreviations $z^{(i)}$ and $T_{(i)}^{(j)}$ for the matrix elements of the z operator and of the induced potential of oscillator (j), respectively. Note that the quantity $T_{(i)}^{(j)}$ is simply the Coulomb interaction energy of oscillators (i) and (j) in the case of unit excitation amplitude. Inserting Eq. (26) into Eq. (18), we obtain a dynamic equation, which determines the excitation amplitudes of the coupled two-level systems for a given strength F and frequency ω of the excitation light

$$u^{(i)}(\omega) = p^{(i)}(\omega) \cdot \left[\frac{-eFz^{(i)}}{2} + \sum_{j \neq i} T_{(i)}^{(j)} u^{(j)}(\omega) \right]. \quad (27)$$

This can be expressed in the form of a complex linear system of equations, if we implicitly assume that $T_{(j)}^{(j)} = 0$ (no self-interaction):

$$\sum_j [\delta_{(i)(j)} - p^{(i)}(\omega) T_{(i)}^{(j)}] u^{(j)}(\omega) = p^{(i)}(\omega) \frac{-eFz^{(i)}}{2}. \quad (28)$$

After solving this system numerically, we will compute the absorption coefficient $\alpha(\omega)$ from the resulting amplitudes $u^{(i)}(\omega)$. In a disordered system the optical power absorbed from the light field is, in principle, a function of the in-plane position. We are, however, not interested in this position dependence. Therefore, we perform in-plane averages over the relevant quantities. This operation is formally denoted by

$$\langle \dots \rangle_{xy} = \Omega^{-1} \int \dots dx dy, \quad (29)$$

where Ω is the lateral system area. In a first step, we calculate the averaged, total space-charge fluctuation of the system:

$$\bar{\rho}(z, \omega) = \left\langle \sum_i \rho^{(i)}(\vec{R}, \omega) \right\rangle_{xy} \quad (30)$$

$$= \sum_i u^{(i)}(\omega) \langle \rho_0^{(i)}(\vec{R}) \rangle_{xy} \quad (31)$$

$$= \sum_i u^{(i)}(\omega) \bar{\rho}_0^{(i)}(z). \quad (32)$$

Here, we have used Eq. (19) and defined an *averaged form factor* $\bar{\rho}_0^{(i)}(z)$ of oscillator (i):

$$\bar{\rho}_0^{(i)}(z) = (-e) \langle \varphi_1^{(i)*}(\vec{R}) \varphi_0^{(i)}(\vec{R}) \rangle_{xy}. \quad (33)$$

At this point it should be remembered that in the above expression the indices 0 and 1 of the single-particle wave functions denote the ground- and first-excited state of dot (i). Each of these states are, in general, x - y -dependent linear combinations of the undisturbed subbands m

$$\varphi_s^{(i)}(\vec{R}) = \sum_m f_m(z) g_m^{(is)}(x, y), \quad (34)$$

Thus, the averaged form factor yields

$$\bar{\rho}_0^{(i)}(z) = (-e) \sum_{mn} f_n(z) f_m(z) \langle g_n^{(i1)*}(x, y) g_m^{(i0)}(x, y) \rangle_{xy} \quad (35)$$

$$= (-e) \sum_{mn} f_n(z) f_m(z) G_{mn}^{(i)}, \quad (36)$$

with the lateral overlap integrals $G_{mn}^{(i)}$. In the case of perfect intradot (intersubband) correlations, we would have

$$g_m^{(is)}(x, y) = \delta_{ms} g^{(i)}(x, y) \quad (37)$$

and the overlap integrals in Eq. (36) would simplify to

$$G_{mn}^{(i)} = \delta_{m0} \delta_{n1} \langle |g^{(i)}(x, y)|^2 \rangle_{xy} = \delta_{m0} \delta_{n1} \Omega^{-1}. \quad (38)$$

In this case, the averaged form factor can be written as

$$\bar{\rho}_0^{(i)}(z) = (-e) \Omega^{-1} f_0(z) f_1(z), \quad (39)$$

which is, due to the orthogonality of the z -subband wave functions, a zero-mean function

$$\int_{-\infty}^{+\infty} dz \bar{\rho}_0^{(i)}(z) = 0. \quad (40)$$

Thus, the induced charge-density fluctuation has a zero-monopole moment. Each oscillator basically represents a localized dipole and, correspondingly, the resulting potential has only a finite range.

We now calculate the ac current connected with the above charge-density fluctuation. The continuity equation

$$\frac{\partial}{\partial z} \bar{j}(z, t) + \frac{\partial}{\partial t} \bar{\rho}(z, t) = 0 \quad (41)$$

links the average induced z current $\bar{j}(z,t)$ with the total space-charge fluctuation. Transforming Eq. (41) into temporal Fourier space and solving for the current yields

$$\bar{j}(z,\omega) = (-i\omega) \int_{-\infty}^z dz' \bar{\rho}(z',\omega). \quad (42)$$

By inserting Eq. (32) we obtain

$$\bar{j}(z,\omega) = (-i\omega) \sum_i u^{(i)}(\omega) \int_{-\infty}^z dz' \bar{\rho}_0(z'). \quad (43)$$

Finally, the zz component of the dynamic conductivity tensor $\sigma_{zz}(\omega)$, the real part of which is proportional to the absorption coefficient $\alpha(\omega)$, follows from the induced current by

$$\sigma_{zz}(\omega) = \frac{1}{F} \int_{-\infty}^{+\infty} dz \bar{j}(z,\omega). \quad (44)$$

Defining the quantity

$$l^{(i)} = \int_{-\infty}^{+\infty} dz \int_{-\infty}^z dz' \bar{\rho}_0^{(i)}(z')/e, \quad (45)$$

which has the dimension of a length, we can express the conductivity in terms of the excitation amplitudes of the localized oscillators

$$\sigma_{zz}(\omega) = \frac{-i\omega e}{F\Omega} \sum_i l^{(i)} u^{(i)}(\omega). \quad (46)$$

In the case of perfect intradot correlations [Eq. (39)] one can easily prove the identity $l^{(i)} = -z^{(i)} = \text{const.}$ Note that since the excitation amplitudes $u^{(i)}(\omega)$ are proportional to the external field strength F (linear response regime), the conductivity $\sigma_{zz}(\omega)$ becomes independent of F . In a similar way, the number of oscillators ($i = 1 \dots N_{\text{osc}}$) increases linearly with the system area Ω . Thus, $\sigma_{zz}(\omega)$ is independent of Ω , too.

IV. MODEL SYSTEM

We applied the above theory to a simple-model system, which has the advantage of facilitating easy evaluation of the matrix elements and convenient numerical implementation. In this model, we consider a planar array of two-level oscillators (dots) of density $n^{(2)}$. Assuming for simplicity that each oscillator is occupied with one electron, $n^{(2)}$ can also be interpreted as the (2D-) electron density. All oscillators are described by wave functions of the same form, however located at different random in-plane positions $\vec{r}_{(i)}$

$$\varphi_m^{(i)}(\vec{R}) = f_m(z) g(\vec{r} - \vec{r}_{(i)}). \quad (47)$$

This z - \vec{r} -separable form with m -independent lateral functions $g(\vec{r})$ captures the essence of the IS correlation effect (case of perfect correlations). Note that the structural (or off-diagonal) disorder is provided here exclusively by the random in-plane distribution of the dot centers.

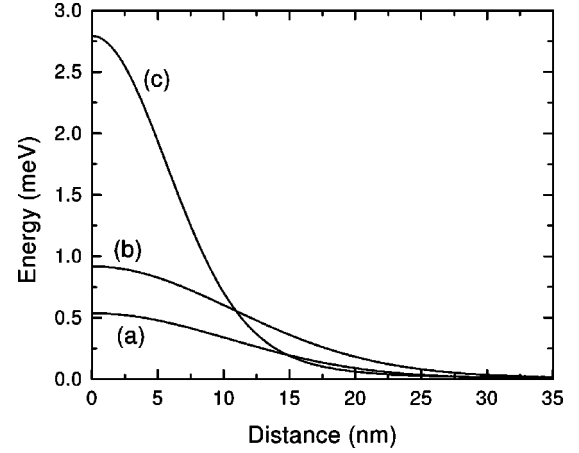


FIG. 1. Coulomb interaction energy $T_{(i)}^{(j)}$ as a function of the interdot distance $r_{(i)(j)}$ in the ‘‘sine-Gauss’’ model system. The parameters were the thickness a of the z -quantum well and the lateral localization radius β^{-1} . Case (a): $a = 10$ nm, $\beta^{-1} = 10$ nm. Case (b): $a = 5$ nm, $\beta^{-1} = 10$ nm. Case (c): $a = 10$ nm, $\beta^{-1} = 5$ nm.

In the longitudinal direction, we assumed an infinite barrier quantum well of thickness a , yielding sine-type z wave functions

$$f_m(z) = \sqrt{2/a} \sin\{(m+1)(\pi/a)[z - (a/2)]\} \quad \text{with } m = 0, 1. \quad (48)$$

In the lateral direction, Gaussian functions have been used

$$g(\vec{r} - \vec{r}_{(i)}) = \frac{\beta}{\sqrt{\pi}} e^{-(\beta|\vec{r} - \vec{r}_{(i)}|)^2/2}, \quad (49)$$

where $\beta = 1/r_{loc}$ is a ‘‘localization parameter.’’

In order to make the effect of the Coulomb interaction as clearly visible as possible, we artificially introduced a box-shaped line broadening into the single-particle levels (diagonal disorder). The transition energy of each dot (i) has thus been detuned from the undisturbed subband separation ϵ_{10} by random shifts, which were equally distributed within the interval $[-\Delta\epsilon_{dis}/2 \dots +\Delta\epsilon_{dis}/2]$. The parameter $\Delta\epsilon_{dis}$ corresponds to the ‘‘inhomogeneous broadening.’’

V. RESULTS AND DISCUSSION

In the following, we present numerical results obtained with the ‘‘sine-Gauss’’-model described above. For the simulations we have typically used $N_{\text{osc}} = 50$ oscillators in a finite system of lateral dimensions $L_x = L_y = \sqrt{N_{\text{osc}}/n^{(2)}}$, with periodic boundary conditions in both directions x and y . The lateral positions $\vec{r}_{(i)}$ of the oscillators have been chosen randomly, with the exception of a minimum distance condition, $r_{(i)(j)} > r_{min}$, to avoid unphysical configurations.

A quantity of central importance is, of course, the Coulomb interaction energy $T_{(i)}^{(j)} = T(r_{(i)(j)})$, which depends on the parameters a and β of the single-particle wave functions. Figure 1 is a plot of the distance dependence of T for various parameter combinations. It shows dipolelike behavior for large distances, but saturates to a finite value at $r_{(i)(j)} = 0$, due to the spatial extension of the charge distributions. Note

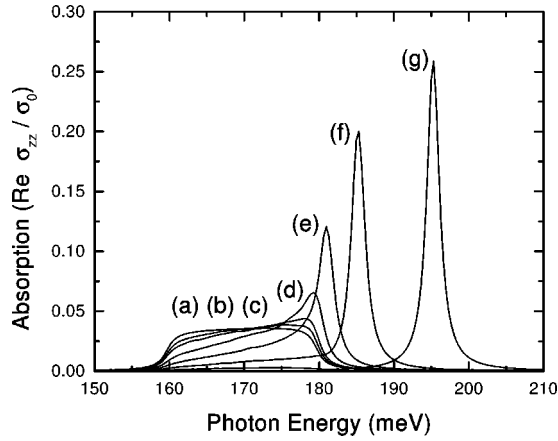


FIG. 2. Intersubband absorption spectrum with diagonal disorder $\Delta\epsilon_{dis}=20$ meV for various 2D-electron densities $n^{(2)}$. The spectrum has been averaged over an ensemble of 100 random configurations, each containing 50 localized oscillators. The other system parameters were as follows: $a=10$ nm, $1/\beta=10$ nm, $\Gamma=1$ meV. Case (a): $n^{(2)}\rightarrow 0$. Case (b): $n^{(2)}=1\times 10^{11}$ cm $^{-2}$. Case (c): $n^{(2)}=2\times 10^{11}$ cm $^{-2}$. Case (d): $n^{(2)}=5\times 10^{11}$ cm $^{-2}$. Case (e): $n^{(2)}=1\times 10^{12}$ cm $^{-2}$. Case (f): $n^{(2)}=2\times 10^{12}$ cm $^{-2}$. Case (g): $n^{(2)}=5\times 10^{12}$ cm $^{-2}$.

that the maximum coupling strength $T(0)$ and the range of interaction r_{max}^{int} [let us define r_{max}^{int} as the distance where T decreases to $T(0)/10$] are mainly determined by the lateral localization radius β^{-1} . For realistic values $\beta^{-1}\approx 10$ nm, however, $T(0)$ is only of order 0.5 meV and r_{max}^{int} is about 30 nm.

In the following, we fix the wave function related parameters to $a=\beta^{-1}=10$ nm and the homogeneous phonon broadening to $\Gamma=1$ meV. For this well thickness, the undisturbed subband separation would be $\epsilon_{10}^{(i)}\approx 170$ meV (infinite barriers).

We now turn to the resulting IS absorption spectrum [the real part of the dynamic conductivity Eq. (46)] of a random array of oscillators. The conductivity is conveniently presented in the natural unit of the Drude value $\sigma_0=n^{(2)}e^2\tau/m^*$, with a phenomenological scattering time related to the homogeneous phonon broadening energy $\tau=\hbar/\Gamma$. The absorption spectrum will, of course, depend on the inhomogeneous disorder broadening $\Delta\epsilon_{dis}$ and the density of oscillators (electrons) $n^{(2)}$.

Figure 2 shows ensemble averaged intersubband spectra for fixed disorder $\Delta\epsilon_{dis}=20$ meV but different electron densities $n^{(2)}$. Case (a) corresponds to the ‘‘dilute limit’’ $n^{(2)}\rightarrow 0$, where the typical nearest-neighbor distance $\bar{r}_{nn}=1/\sqrt{n^{(2)}}$ exceeds the range of interaction r_{max}^{int} and thus Coulomb coupling can be neglected. In this case, the spectrum is, of course, only determined by the single-particle properties and reflects the specific distribution of the individual transition energies $\hbar\Delta\omega_{10}^{(i)}$. Therefore, in our model we obtain a broad, box-shaped absorption band of width $\Delta\epsilon_{dis}$, centered around the IS energy separation $\epsilon_{10}\approx 170$ meV of the ‘‘undisturbed’’ z -quantum well. The spectrum remains essentially unchanged as long as $n^{(2)}$ is smaller than the critical density $n_{crit}^{(2)}=1/(r_{max}^{int})^2$, which is about 1.1×10^{11} cm $^{-2}$ for our case of $r_{max}^{int}=30$ nm.

In cases (b)–(d), corresponding to $n^{(2)}=1.0\dots 5.0$

$\times 10^{11}$ cm $^{-2}$, the effect of the electron-electron interaction already becomes clearly visible in the spectrum. A peak is formed on the high-energy side of the single-particle band at the cost of absorption in the low-energy range.

This trend is continued in cases (e) and (f). The peak becomes more pronounced, growing in height, reducing its width and shifting to higher energies. Note, however, that at this electron density the presence of disorder could still be deduced from the spectrum by the long low-energy tail.

At even higher densities [case (g)], the blueshift and change of shape of the peak become extremely pronounced. The line shape approaches a Lorentzian of a width limited only by the homogeneous phonon broadening Γ . Finally, there remains almost no trace of the strong disorder in the spectrum.

It is clear that the density dependent blueshift $\Delta\hbar\omega(n^{(2)})$ of the absorption peak in Fig. 2 is a manifestation of the well-known depolarization effect, here realized in a system of strongly localized states. It is also apparent from the characteristic line distortion that the sharp absorption peak corresponds to a collective response of all electrons to the external optical field.

However, it is desirable to understand in greater detail, how the localized oscillators ‘‘cooperate’’ in the collective mode. For a given excitation frequency ω , the dynamic microstate of the system is completely described by the modulus and phase of the complex excitation amplitudes $u^{(i)}(\omega)$ of the individual oscillators. We have, therefore, analyzed a specific configuration of 50 dots and visualized the in-plane distribution of the oscillator amplitudes in Fig. 3. All parameters have been chosen like in the case of Fig. 2(f), i.e., the electron density was $n^{(2)}=2\times 10^{12}$ cm $^{-2}$. The centers of the circles in Fig. 3 indicate the localization positions of each oscillator. The modulus and phase of an oscillator amplitude are represented by the size of the circle and the orientation of the arrow, respectively. The circle diameter d is a linear measure of the excitation level, $d=d_0+c|u^{(i)}(\omega)|$, but a minimum size d_0 has been added for graphical reasons. In case of in-phase oscillation with the external field ($\Delta\varphi=0$), the arrow points to the right, while out-of-phase motion ($\Delta\varphi=-\pi$) would be represented by an arrow pointing to the left.

Part (a) corresponds to photon energy $\hbar\omega=180$ meV, which is in the low-energy tail of the IS resonance Fig. 2(f). It can be seen that only a few oscillators are strongly excited at this frequency. There is a broad distribution of phases, in such a way that similar phases are spatially grouped together. Neighboring electrons mutually adapt their phases, thus forming coherently oscillating clusters. The extension of these clusters becomes larger, if the photon energy approaches the peak energy of the absorption maximum.

Part (b) belongs to photon energy $\hbar\omega=185$ meV, which is close to the peak of the collective resonance. While the individual oscillators still have different excitation levels, now the phase distribution is much smaller: A single-coherent cluster has percolated over the (finite) system and all electrons oscillate in phase with each other. This is the form of cooperation, which gives rise to the high value of total absorption.

For higher photon energies this collective phase adjustment becomes even more pronounced, with all $\Delta\varphi$ finally approaching the value $-\pi$ (like the out-of-phase motion of a

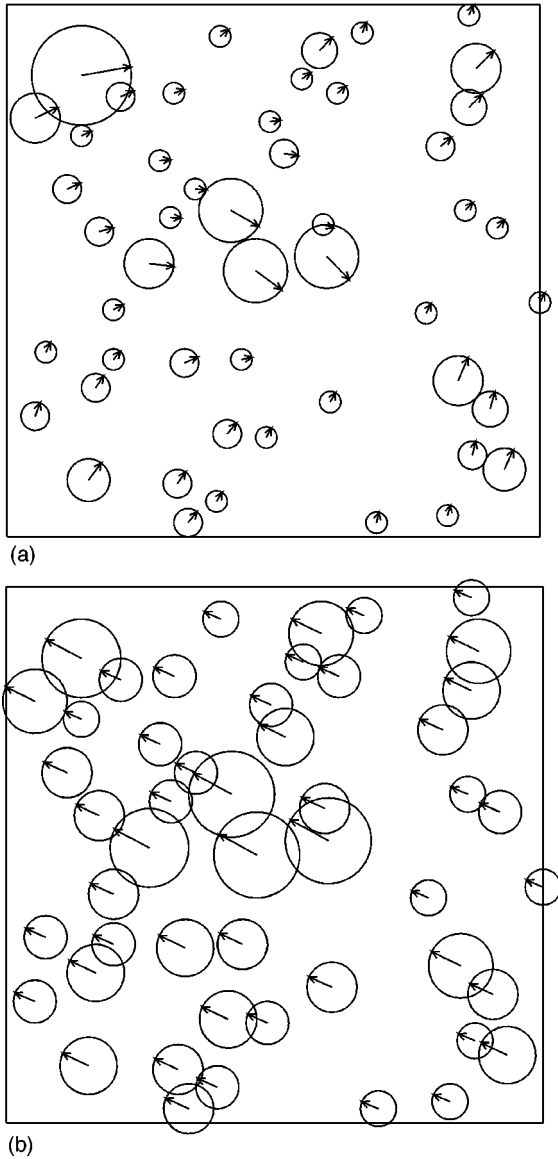


FIG. 3. Visualization of the individual oscillator's complex excitation amplitudes for a specific configuration at two different photon energies. The system parameters were as in Fig. 2(f), i.e., $n^{(2)} = 2 \times 10^{12} \text{ cm}^{-2}$. The centers of the circles denote the in-plane positions of the natural quantum dots in the simulation area. Modulus and phase of their amplitudes are represented by the size of the circles and the orientation of the arrows, respectively. In-phase oscillation corresponds to an arrow pointing to the right ($\Delta\varphi=0$), out-of-phase motion is depicted by an arrow pointing to the left ($\Delta\varphi=-\pi$). Case (a): Before resonance ($\hbar\omega=180 \text{ meV}$). Case (b): Close to resonance ($\hbar\omega=187 \text{ meV}$).

harmonic oscillator driven far beyond the resonance frequency). However, the excitation levels are rapidly decreasing after $\hbar\omega$ has passed the peak value.

VI. CONCLUSION

In the following, we summarize the key points of this paper, relate the results to other parts of semiconductor physics and discuss possible future extensions of our theory.

In this paper, we have investigated IS absorption of z-polarized light in a quasi-2D electron layer with strong

lateral disorder. Such a spatially inhomogeneous electron film has to be described by in-plane localized single-particle wave functions. Since the IS transitions occur between correlated pairs of such states, the system can be viewed as a set of distinct oscillators. These have resonance frequencies distributed around the subband separation of the corresponding ideal layer ϵ_{10} , but are fluctuating on a scale $\Delta\epsilon_{dis}$ (inhomogeneous broadening), which is determined by the disorder and IS correlation effects. Each individual oscillator contributes to the total IS spectrum a comparatively narrow absorption line. Its (homogeneous) width Γ is exclusively determined by the phonon (or photon) emission rate and the oscillator strength depends on the overlap of the involved lateral wave functions. Thus, in a single-particle picture (or at not too high-electron density), the IS spectrum is a linear superposition of many phonon-broadened resonances and the final line shape will, in general, be neither Gaussian, nor Lorentzian. This picture is in agreement with recent spectral hole burning experiments, which demonstrate that the inhomogeneous broadening $\Delta\epsilon_{dis}$ can be larger than the fundamental homogeneous linewidth Γ , even in modulation doped quantum wells.

Assuming the above scenario, we have formulated a theory of dynamic electron-electron interaction effects on the intersubband resonance, which is completely based on localized single-particle states. For this purpose, we calculated the linear response of an interacting set of N two-level oscillators, subject to both the external optical field and the induced, selfconsistent Hartree field. For given frequency of the incoming light field, the theory describes the dynamic microstate of the system by a simple, linear system of N equations, determining the individual (complex) excitation amplitudes of the oscillators. The laterally averaged IS absorption spectrum follows then essentially from a weighted sum of these amplitudes.

We have numerically evaluated our theory for a simplified model system with "sine-Gauss" single-particle states and a box-shaped IS absorption spectrum (without electron-electron interactions). In this model, the Coulomb coupling of neighboring oscillators is basically a dipole-dipole interaction of finite range r_{max}^{int} . The many-particle effects have then been turned on by gradually increasing the electron density $n^{(2)}$ or, in other words, by decreasing the average distance \bar{r}_{nn} between the localized oscillators, until $\bar{r}_{nn} \leq r_{max}^{int}$.

The simulations show a drastic, qualitative change of the IS spectrum as a function of $n^{(2)}$. Starting from the broad, box-shaped absorption band at $n^{(2)} \rightarrow 0$ (reflecting the single-particle properties), the spectrum gradually evolves to an approximately Lorentzian line (corresponding to a many-particle excitation of the whole system). With increasing electron density, this resonance peak becomes narrower and shifts to higher energies, which is analogous to the case of quasi-two-dimensional systems with laterally extended states. This collective effect could be explained by a mutual phase adaption of the Coulomb-coupled localized oscillators.

This results demonstrates, that the "true," inhomogeneous broadening in a disordered system can be completely "screened out" by the dynamic many-particle interactions and thus may remain unobserved in an IS experiment performed at fixed electron density. Especially, the Lorentzian

line shape of the IS spectrum allows in general no statements about the nature of the line broadening.

VII. OUTLOOK

Our model system closely resembles an array of self-organized $\text{In}_x\text{Ga}_{1-x}\text{As}$ quantum dots, at least with respect to the form of the single-particle wave functions (compare Refs. 28, 29, and 30 and references therein). Actually, these systems are very interesting candidates for the study of static²⁷ and dynamic many-electron correlation effects. Yet there are also two major differences.

First, in typical $\text{In}_x\text{Ga}_{1-x}\text{As}$ dots the various internal quantum states are *lateral modes* (e.g., corresponding to the spectrum of a two-dimensional harmonic oscillator), which all belong to the same z -subband. When intraband absorption experiments are performed with such dot-arrays, consequently, light is polarized parallel to the layers. Nevertheless, the dynamic depolarization effect studied in this paper is also effective between electrons oscillating in the lateral direction and may cause a similar line shift and narrowing. We are, thus, working on an analogous theory for lateral polarization.

On the other hand, the situation studied in this paper may be realized, for example, in strain-induced dots. In this concept, an ordinary quantum well is used to provide the (adjustable) z quantization, while the lateral confinement results from the strain field of a neighboring layer of dots. Thus, in a sufficiently wide quantum well several longitudinal modes could be created, each associated with a similar set of (correlated) lateral modes.

Another major difference between our model and $\text{In}_x\text{Ga}_{1-x}\text{As}$ dot arrays lies in the in-plane dot density. For typical growth conditions the resulting densities may be too low to observe drastic effects of the interdot coupling. The situation might be improved by charging each dot with more than one electron. However, this would require the inclusion of intradot Coulomb effects (see below).

Thus, our theory basically applies to strongly disordered quasi-2D systems, like δ -doped layers or modulation doped quantum wells with thin spacer layer. To directly compare theoretical results with experimental data, it is unnecessary to use realistic, disordered quantum states, as they result from exact diagonalization studies. Such simulations are now in progress.

Another class of systems, in which dynamic interaction effects between localized oscillators should play an important role, are disordered 2D systems subject to a strong-magnetic field in z direction.³¹ The density of states is then condensed into several, broadened Landau peaks. Except at the center of each Landau peak, the wave functions are lat-

erally localized and there should exist strong correlations between corresponding states of different Landau bands (because electrons in different Landau bands “see” the same lateral disorder). Transitions are induced between such correlated states in cyclotron resonance experiments. Therefore, there is a strong analogy to the case treated in this paper.

In the present version of the theory we have treated the oscillators as two-level systems, assuming that each initial state $|i0\rangle$ is connected (by the optical dipole operator p_z) to only one correlated final state $|i1\rangle$. In actual disordered systems, however, there can exist several final states $|i(m)\rangle, m=1 \dots M$, with some of the transition energies $\epsilon_{m0}^{(i)}$ being similar and close to the excitation photon energy. In such a case, all the involved quantum states must be retained in Eq. (13) and one obtains a system of interacting $(M+1)$ -level systems. This extension would not affect the essence of the theory, but can of course have drastic consequences for the resulting spectral shape. Also higher subbands can have an effect on the 0-1 resonance, even if they are far separated energetically.

A difficulty arises concerning the Pauli principle, if different electrons share the same one-particle states, i.e., in the case of multiple occupancy of the quantum dots. Then, of course, the intradot electron-electron interaction (“Coulomb blockade”) becomes very important. This problem is closely connected with electron spin, which has been neglected in the present work. In such a case, each dot must be described by a suitable N -particle wave function, which should still be tractable for small N .

From the theory of the intersubband resonance in systems with laterally extended states it is well known that the depolarization blueshift is partly cancelled by the exchange-correlation effects (vertex corrections, or excitonic final-state interactions).^{7,8,10} It still remains to be clarified which role such effects play in the strongly localized regime, where the wave functions belonging to different dots have typically a very small spatial overlap. Thus, exchange effects *between* the dots are suppressed and the corresponding Coulomb integrals are expected to be small.

Finally, it should be mentioned that in the present stage, the electron-phonon interaction has been included only phenomenologically by a homogeneous broadening energy. We are now working towards an explicit calculation of electron-phonon scattering times on the basis of realistic, localized electron states.

ACKNOWLEDGMENT

One of the authors (C.M.) would like to thank the Deutsche Forschungsgemeinschaft DFG for financial support.

¹B. Levine, K. Choi, C. Bethea, J. Walker, and R. Malik, Appl. Phys. Lett. **50**, 1092 (1987).

²N. Vodjani, B. Vinter, V. Berger, E. Bockenhoff, and E. Costard, Appl. Phys. Lett. **59**, 555 (1989).

³J. Faist, F. Capasso, L. Sivco, C. Sirtori, A. Hutchinson, and A. Cho, Science **264**, 553 (1994).

⁴Ph. Boucaud, F.H. Julien, D.D. Yang, J.-M. Lourtioz, E. Rosencher, Ph. Bois, and J. Nagle, Appl. Phys. Lett. **57**, 215 (1990).

⁵J.B. Khurgin and S. Li, Appl. Phys. Lett. **62**, 126 (1993).

⁶T. Ando, Z. Phys. B: Condens. Matter **26**, 263 (1977).

⁷T. Ando, A.B. Fowler, and F. Stern, Rev. Mod. Phys. **54**, 437 (1982).

⁸W. Bloss, J. Appl. Phys. **66**, 3639 (1989).

⁹E. Batke, G. Weimann, and W. Schlapp, Phys. Rev. B **43**, 6812 (1991).

¹⁰D.E. Nikonov, A. Imamoglu, L.V. Butov, and H. Schmidt, Phys. Rev. Lett. **79**, 4633 (1997).

¹¹R.J. Warburton, K. Weilhammer, J. Kotthaus, M. Thomas, and H. Kroemer, Phys. Rev. Lett. **80**, 2185 (1998).

- ¹²M. Zaluzny, Phys. Rev. B **43**, 4511 (1991).
- ¹³C. Gauer, A. Wixforth, J.P. Kotthaus, M. Kubisa, W. Zawadzki, B. Brar, and H. Kroemer, Phys. Rev. Lett. **74**, 2772 (1995).
- ¹⁴K. Craig, B. Galdrikian, J.N. Heyman, A.G. Markelz, J.B. Williams, M.S. Sherwin, K. Campman, P.F. Hopkins, and A.C. Gossard, Phys. Rev. Lett. **76**, 2382 (1996).
- ¹⁵R.J. Warburton, C. Gauer, A. Wixforth, J.P. Kotthaus, B. Brar, and H. Kroemer, Phys. Rev. B **53**, 7903 (1996).
- ¹⁶R. Warburton, C. Gauer, A. Wixforth, J.P. Kotthaus, B. Brar, and H. Kroemer, Superlattices Microstruct. **19**, 365 (1996).
- ¹⁷Paul von Allmen, M. Berz, F.K. Reinhart, and G. Harbeke, Semicond. Sci. Technol. **3**, 1211 (1988).
- ¹⁸T. Ando, J. Phys. Soc. Jpn. **54**, 2671 (1985).
- ¹⁹E.B. Dupont, D. Delacourt, D. Papillon, J.P. Schnell, and M. Papuchon, Appl. Phys. Lett. **60**, 2121 (1992).
- ²⁰J. Faist, F. Capasso, C. Sirtori, D.L. Sivco, A.L. Hutchinson, Sung Nee G. Chu, and A.Y. Cho, Appl. Phys. Lett. **65**, 94 (1994).
- ²¹K.L. Campman, H. Schmidt, A. Imamoglu, and A.C. Gossard, Appl. Phys. Lett. **69**, 2554 (1996).
- ²²J. Faist, C. Sirtori, F. Capasso, L. Pfeiffer, and K.W. West, Appl. Phys. Lett. **64**, 872 (1994).
- ²³G. Beadie, W.S. Rabinovich, D.S. Katzer, and M. Goldberg, Phys. Rev. B **55**, 9731 (1997).
- ²⁴S.R. Schmidt, J. Kaiser, and A. Seilmeier, Verh. Dtsch. Phys. Ges. **34**, 771 (1999), Paper HL 29.3.
- ²⁵C. Metzner, M. Hofmann, and G.H. Döhler, Phys. Rev. B **58**, 7188 (1998).
- ²⁶C. Metzner, M. Hofmann, and G.H. Döhler, Superlattices Microstruct. **25**, 239 (1999).
- ²⁷C. Metzner, G. Yusa, and H. Sakaki, Superlattices Microstruct. **25**, 537 (1999).
- ²⁸M. Fricke, A. Lorke, J.P. Kotthaus, G. Medeiros-Ribeiro, and P.M. Petroff, Europhys. Lett. **36**, 197 (1996).
- ²⁹R.J. Warburton, C.S. Dürr, K. Karrai, J.P. Kotthaus, G. Medeiros-Ribeiro, and P.M. Petroff, Phys. Rev. Lett. **79**, 5282 (1997).
- ³⁰R.J. Warburton, B.T. Miller, C.S. Dürr, C. Bödefeld, K. Karrai, J.P. Kotthaus, G. Medeiros-Ribeiro, P.M. Petroff, and S. Huan, Phys. Rev. B **58**, 16 221 (1998).
- ³¹U. Merkt, Phys. Rev. Lett. **76**, 1134 (1996).